Nonperturbative density-functional theories of classical nonuniform systems

James F. Lutsko and Marc Baus
Faculté des Sciences, Campus Plaine, Code Postal 231, Université Libre de Bruxelles, B-1050 Brussels, Belgium
(Received 6 February 1990)

We propose an approximation to the density-functional theory of classical nonuniform systems that reproduces all the formal properties of the free energy and requires only the direct correlation function of the uniform system as input. By introducing additional assumptions into this theory a direct relation can be established with most of the existing nonperturbative theories. When the theory is worked out for the case of the hard-sphere solid, very good agreement is found with the computer simulations. The free energies, pressures, and fluid-solid coexistence data are reproduced to within the error bars of the simulations. The theory also predicts stable bcc and sc phases that could play a role in the final nucleation of the equilibrium fcc phase.

I. INTRODUCTION

The density-functional (DF) theory of classical nonuniform systems[1] has become an increasingly popular tool to study the thermodynamic (and to a lesser extent also the structural) properties of liquid-vapor,[2] liquid-solid[3] first-order phase transitions and the associated interfaces. The DF theory itself is essentially a direct-correlation-function- (DCF) based approach to equilibrium statistical mechanics.[4] Because the DCF is relatively insensitive to the details of the interaction potential,[4] it has proven to be a good starting point for developing approximation schemes. The same is thus also true for the DF theory. Approximate DF theories usually aim at describing the (thermodynamic) properties of the nonuniform system (fluid interface, solid, etc.), characterized by a nonuniform one-particle density, in terms of the (structural) properties of the uniform system (usually the bulk liquid), characterized by a uniform one-particle density, the latter properties are assumed to be known. For concreteness, we henceforth will speak of the nonuniform system as the solid and the uniform system as the liquid (or fluid) although many other situations (e.g., liquid crystals[5]) can be considered equally well. In these terms then, the early DF theories are all based on a perturbative expansion[6] of the free energy of the solid around the free energy of the liquid. Very little care was given to the theoretical foundation of this expansion and it is only recently that this whole procedure was called into question.[6,7] Several authors also proposed nonperturbative approaches to the DF theory but again very little attention has been paid to the theoretical foundation behind these distinct proposals. In the present investigation we focus our attention on these theoretical questions and bring to the foreground the more successful ideas. In doing so, we will formulate an approximate DF theory that allows us to establish various relations between some of the earlier proposals.

In Sec. II we first recall some of the necessary DF relations. The various approximate (nonperturbative) DF theories will be considered in Sec. III. The results obtained from these theories will be discussed in Sec. IV for the particular case of the hard-sphere (HS) solid. Our conclusions follow in Sec. V.

II. THE BASIC DF RELATIONS

We consider a classical equilibrium system enclosed, at the inverse temperature $\beta=1/k_BT$, in a vessel of volume V, and corresponding to an (average) number of particles ρV, where ρ is the (average) number density resulting from spatially averaging the local density $\rho(\mathbf{r})$ over the volume V:

$$\rho=\frac{1}{V}\int d\mathbf{r}\,\rho(\mathbf{r})\ . \tag{2.1}$$

Here and below, any implicit dependence on T and V [of, e.g., $\rho(\mathbf{r})$] will not be indicated explicitly. The quantity of interest is the (Helmholtz) free energy F of this system. It depends (besides on T and V) on the density, which is the variable of major concern here.

For the *solid* (s), which is our prototype of nonuniform system, the density is nonuniform $\rho_s(\mathbf{r})$ and the dependence of F on $\rho_s(\mathbf{r})$ is thus a functional dependence. We will indicate this by square brackets[1] as $F=F[\rho_s]$, indicating hereby that F depends on $\rho_s(\mathbf{r})$ for all spatial arguments $\mathbf{r}$ belonging to V. It consists of three terms, $F=F_{\rm id}+F_{\rm ext}+F_{\rm ex}$: the ideal-gas contribution $F_{\rm id}$,

$$F_{\rm id}[\rho_s]=\beta^{-1}\int d\mathbf{r}\rho_s(\mathbf{r})\{\ln[\Lambda^3\rho_s(\mathbf{r})]-1\}\ , \tag{2.2}$$

with Λ being the thermal wavelength, the contribution $F_{\rm ext}$ from the external field $\varphi_s(\mathbf{r})$,

$$F_{\rm ext}[\rho_s]=\int d\mathbf{r}\,\rho_s(\mathbf{r})\varphi_s(\mathbf{r})\ , \tag{2.3}$$

and the excess term $F_{\rm ex}$ stemming from the interatomic interactions, which is sometimes written as

$$F_{\rm ex}[\rho_s]=\int d\mathbf{r}\,\rho_s(\mathbf{r})\psi_{\rm ex}(\mathbf{r};[\rho_s]) \tag{2.4}$$

introducing hereby a local excess free energy per particle $\psi_{\rm ex}(\mathbf{r};[\rho_s])$. This quantity should not be confused with the true excess free energy per particle $\phi_{\rm ex}[\rho_s]$:

$$\phi_{ex}[\rho_s]=F_{ex}[\rho_s]/\rho_s V \tag{2.5a}$$

$$=\int d\mathbf{r}\,\rho_s(\mathbf{r})\psi_{ex}(\mathbf{r};[\rho_s])\Big/\int d\mathbf{r}'\rho_s(\mathbf{r}')\ , \tag{2.5b}$$

where according to Eq. (2.1) $\rho_s V=\int d\mathbf{r}\rho_s(\mathbf{r}')$ is the (average) number of particles and ρ_s the average density of the solid.

For the *liquid* (l), which corresponds here to the uniform phase, the density is uniform ρ_l and the above functional dependence becomes an ordinary dependence which we indicate, as usual, as $F=F(\rho_l)$. The above equations [(2.2)–(2.4)] then reduce to

$$F_{id}(\rho_l)=\beta^{-1}V\rho_l\{\ln(\Lambda^3\rho_l)-1\}\ , \tag{2.6}$$

$$F_{ext}(\rho_l)=0\ , \tag{2.7}$$

$$F_{ex}(\rho_l)=V\rho_l\psi_{ex}(\rho_l)\ , \tag{2.8}$$

whereas Eq. (2.5) reduces to $\phi_{ex}(\rho_l)=\psi_{ex}(\rho_l)$, while (2.7) results from $\varphi_l(\mathbf{r})\equiv 0$, as is appropriate for a translationally invariant or uniform bulk liquid. Notice, however, that in Eq. (2.3) we are not allowed to put $\varphi_s(\mathbf{r})\equiv 0$, since $\varphi_s(\mathbf{r})$ is necessary in order to define the functionals uniquely[1] by fixing completely the nature of $\rho_s(\mathbf{r})$, e.g., the orientation of the crystalline axes and the other symmetry-breaking characteristics. The role played by the external field is thus more subtle for the solid than for the liquid. Here we will assume, as usual, that once the thermodynamic limit has been taken (which will be understood henceforth) all intensive properties no longer depend explicitly on $\varphi_s(\mathbf{r})$, except of course for those features already taken into account via $\rho_s(\mathbf{r})$. We will therefore delete F_{ext} from our considerations. Everything thus boils down to obtaining a more explicit expression of F_{ex}, the only unknown quantity encountered as yet. A crucial role is played then by the fact that $F_{ex}[\rho_s]$ is a generating functional[1] of the successive DCF, defined according to the following chain rule ($n=1,2,\ldots$):

$$C_n(\mathbf{r}_1,\ldots,\mathbf{r}_n;[\rho_s])=\frac{\delta C_{n-1}(\mathbf{r}_1,\ldots,\mathbf{r}_{n-1};[\rho_s])}{\delta\rho_s(\mathbf{r}_n)} \tag{2.9a}$$

$$=\frac{\delta^n C_0[\rho_s]}{\delta\rho_s(\mathbf{r}_1)\cdots\delta\rho_s(\mathbf{r}_n)}\ , \tag{2.9b}$$

where, for brevity, we have put $C_0[\rho_s]\equiv-\beta F_{ex}[\rho_s]$. The differential relations (2.9) can also be "inverted" with the help of functional integrations in density space. If we parametrize the density variable as $\rho_\lambda(\mathbf{r})$, with $\lambda=0$ corresponding to some known reference (r) density, $\rho_0(\mathbf{r})\equiv\rho_r(\mathbf{r})$, and $\lambda=1$ to the actual solid density, $\rho_1(\mathbf{r})\equiv\rho_s(\mathbf{r})$, then we obtain from (2.9) the equivalent integral relations

$$C_0[\rho_s]=C_0[\rho_r]+\int d\mathbf{r}\int_0^1 d\lambda\,\rho'_\lambda(\mathbf{r})C_1(\mathbf{r};[\rho_\lambda])$$

$$=C_0[\rho_r]+\int d\mathbf{r}\int_0^1 d\lambda\rho'_\lambda(\mathbf{r})C_1(\mathbf{r};[\rho_r]) \tag{2.10a}$$

$$+\int d\mathbf{r}\int d\mathbf{r}'\int_0^1 d\lambda\int_0^\lambda d\lambda'\rho'_\lambda(\mathbf{r})\rho'_{\lambda'}(\mathbf{r})\times C_2(\mathbf{r},\mathbf{r}';[\lambda'\rho_s]) \tag{2.10b}$$

where we have set $\rho'_\lambda(\mathbf{r})\equiv\partial\rho_\lambda(\mathbf{r})/\partial\lambda$ and have stopped at the C_2 level since of all the C_n's defined by Eq. (2.9) only the ordinary (Ornstein-Zernike) DCF C_2 is known to some extent.[4] We will therefore designate C_2 henceforth as "the" DCF: $C(\mathbf{r},\mathbf{r}';[\rho_s])=C_2(\mathbf{r},\mathbf{r}';[\rho_s])$. Notice also that because of the uniqueness of these functionals[1] one can simplify (2.10) by taking a linear path in density space:

$$\rho_\lambda(\mathbf{r})=\rho_r(\mathbf{r})+\lambda[\rho_s(\mathbf{r})-\rho_r(\mathbf{r})]\ , \tag{2.11a}$$

$$\rho'_\lambda(\mathbf{r})=\rho_s(\mathbf{r})-\rho_r(\mathbf{r})\equiv\Delta\rho(\mathbf{r})\ , \tag{2.11b}$$

while for the double λ integral in (2.10b) one can use the identity

$$\int_0^1 d\lambda\int_0^\lambda d\lambda' h(\lambda')=\int_0^1 d\lambda(1-\lambda)h(\lambda)\ , \tag{2.12}$$

valid for any $h(\lambda)$. The central relation between $F_{ex}[\rho_s]$ and the DCF reads thus in these notations:

$$C(\mathbf{r},\mathbf{r}';[\rho_s])=-\frac{\delta^2\beta F_{ex}[\rho_s]}{\delta\rho_s(\mathbf{r})\delta\rho_s(\mathbf{r}')}\ , \tag{2.13}$$

which is the differential form corresponding to (2.9b) with $n=2$, or

$$\beta F_{ex}[\rho_s]=-\int d\mathbf{r}\int d\mathbf{r}'\int_0^1 d\lambda\int_0^\lambda d\lambda'\rho_s(\mathbf{r})\rho_s(\mathbf{r}')\times C(\mathbf{r},\mathbf{r}';[\lambda'\rho_s])\ , \tag{2.14}$$

which is the integral form corresponding to (2.10b) for $\rho_r(\mathbf{r})\equiv 0$, which fixes the integration "constants" in (2.10b) as $C_0[0]=0$, $C_1(\mathbf{r},[0])=0$. Notice that Eq. (2.14) is indeed of the form assumed in Eq. (2.4).

For the liquid these fundamental relations [(2.13) and (2.14)] become

$$C(|\mathbf{r}-\mathbf{r}'|;\rho_l)=-\left.\frac{\delta^2\beta F_{ex}[\rho_s]}{\delta\rho_s(\mathbf{r})\delta\rho_s(\mathbf{r}')}\right|_{\rho_s(\mathbf{r})=\rho_l}\ , \tag{2.15}$$

$$\beta F_{ex}(\rho_l)=-V\rho_l^2\int d\mathbf{r}\int_0^1 d\lambda\int_0^\lambda d\lambda' C(|\mathbf{r}|;\lambda'\rho_l)\ , \tag{2.16}$$

where, in the differential relation (2.15), the uniform limit $\rho_s(\mathbf{r})\to\rho_l$ has to be taken after the functional derivatives. Notice also that the integral form (2.16) is equivalent to the usual relation

$$\beta F_{ex}(\rho_l)=-V\int d\mathbf{r}\int_0^{\rho_l}d\rho\int_0^\rho d\rho' C(|\mathbf{r}|;\rho')\ , \tag{2.17}$$

resulting from integrating the compressibility equation of state.[4] In the form of Eq. (2.17) the similarity with (2.14) is quite striking: in (2.17) the liquid is reached by integrating the DCF in density space from $\rho=0$ to $\rho=\rho_l$ along a uniform density path whereas in (2.14) the solid is reached similarly by integrating from $\rho(\mathbf{r})=0$ to $\rho(\mathbf{r})=\rho_s(\mathbf{r})$ along a nonuniform density path. As an alternative one can use Eqs. (2.10)–(2.12) with the liquid as a reference state $\rho_r(\mathbf{r})\equiv\rho_l$ leading to

$$\beta F_{\rm ex}[\rho_s]=\beta F_{\rm ex}(\rho_l)+\beta V(\rho_s-\rho_l)\mu_{\rm ex}(\rho_l)-\int d\mathbf{r}\int d\mathbf{r}'\int_0^1 d\lambda(1-\lambda)C(\mathbf{r},\mathbf{r}';[\rho_l+\lambda(\rho_s-\rho_l)])(\rho_s(\mathbf{r})-\rho_l)(\rho_s(\mathbf{r}')-\rho_l)\ , \tag{2.18}$$

where $\mu_{\rm ex}(\rho_l)$ is the excess chemical potential of the liquid.[1] Equation (2.18) now has the formal appearance of a perturbation expansion of the excess free energy of the solid around that of the liquid. Taylor expanding the λ integral of (2.18) and using (2.9) one obtains

$$\beta F_{\rm ex}[\rho_s]=\beta F_{\rm ex}(\rho_l)+\beta V(\rho_s-\rho_l)\mu_{\rm ex}(\rho_l)-\sum_{n=0}^{\infty}\frac{1}{(2+n)!}\int d\mathbf{r}_1,\ldots,d\mathbf{r}_{n+2}C_{n+2}(\mathbf{r}_1,\ldots,\mathbf{r}_{n+2};\rho_l)\times(\rho_s(\mathbf{r}_1)-\rho_1)\cdots(\rho_s(\mathbf{r}_{n+2})-\rho_l)\ , \tag{2.19}$$

which is the thermodynamic perturbation expansion at the basis of all perturbative DF theories. This perturbation series is usually truncated at the second-order or C_2 level:

$$\beta F_{\rm ex}[\rho_s]=\beta F_{\rm ex}(\rho_l)+\beta V(\rho_s-\rho_l)\mu_{\rm ex}(\rho_l)-\frac{1}{2}\int d\mathbf{r}\int d\mathbf{r}'C(\mathbf{r}-\mathbf{r}';\rho_l)(\rho_s(\mathbf{r})-\rho_l)\times(\rho_s(\mathbf{r}')-\rho_l)+\cdots\ , \tag{2.20}$$

as in the original Ramakrishnan-Yussouff theory.[8] Recently, it has become clear however that the convergence of the expansion (2.19), and hence of all perturbative DF theories, is quite questionable.[6,7] From now on we will therefore consider only the nonperturbative DF theories based on the unexpanded expressions (2.14) or (2.18).

III. THE NONPERTURBATIVE DF THEORIES

The central idea underlying all the approximate DF theories is, in our opinion, that it is possible to obtain good thermodynamic (and to a lesser extent also structural) data for the solid (or any other nonuniform system) by using only the structural (and hence also the thermodynamic) data of the liquid (or the uniform system) as input. This (at first sight quite surprising) possibility is brought about by the similarity of the thermodynamic properties (such as the equation of state) of the two otherwise quite different condensed phases. The quality of the results obtained in this way depends strongly on how this basic idea is implemented in practice. As far as we can see there are essentially two ways of performing such a mapping of the solid onto some "effective" liquid.

(i) *Thermodynamic mapping.* One can map the unknown excess free energy of the solid $F_{\rm ex}[\rho_s]$ or better the corresponding intensive property $\phi_{\rm ex}[\rho_s]=F_{\rm ex}[\rho_s]/\rho_s V$ the excess free-energy per particle, onto that of some effective liquid $\phi_{\rm ex}(\rho_l)=F_{\rm ex}(\rho_l)/\rho_l V$ by writing

$$\phi_{\rm ex}[\rho_s]=\phi_{\rm ex}(\hat{\rho}_1)\ , \tag{3.1}$$

where $\hat{\rho}_1$ is the (uniform) density of the effective liquid which is used to represent the solid of density $\rho_s(\mathbf{r})$. One can reconstruct then the total free energy $F[\rho_s]$ by adding $F_{\rm id}[\rho_s]$ of Eq. (2.2) to $F_{\rm ex}[\rho_s]$ obtained from Eq. (3.1). Let us examine for the consequences of Eq. (3.1). The density of the effective liquid $\hat{\rho}_1$ is seen from Eq. (3.1) to become a functional of the density of the solid $\rho_s(\mathbf{r})$:

$$\hat{\rho}_1=\hat{\rho}_1[\rho_s]\ . \tag{3.2}$$

The nature of this functional relation can be partially resolved by returning to the exact relations (2.14) and (2.16). In terms of these relations Eq. (3.1) can be rewritten as

$$\frac{1}{\rho_s V}\int d\mathbf{r}\int d\mathbf{r}'\int_0^1 d\lambda\int_0^{\lambda}d\lambda'\rho_s(\mathbf{r})\rho_s(\mathbf{r}')C(\mathbf{r},\mathbf{r}';[\lambda'\rho_s])=\hat{\rho}_1\int d\mathbf{r}\int_0^1 d\lambda\int_0^{\lambda}d\lambda' C(|\mathbf{r}|;\lambda'\hat{\rho}_1)\ , \tag{3.3}$$

where $C(\mathbf{r},\mathbf{r}';[\rho_s])$ denotes the DCF of the solid of density $\rho_s(\mathbf{r})$ and $C(|\mathbf{r}-\mathbf{r}'|;\hat{\rho}_1)$ the DCF of the liquid of density $\hat{\rho}_1$. The functional relation (3.2) can now be made more explicit by rewriting Eq. (3.3) as

$$\hat{\rho}_1[\rho_s]=\frac{1}{\rho_s V}\int d\mathbf{r}\int d\mathbf{r}'\rho_s(\mathbf{r})\rho_s(\mathbf{r}')w(\mathbf{r},\mathbf{r}';[\rho_s])\ , \tag{3.4a}$$

$$w(\mathbf{r},\mathbf{r}';[\rho_s])=\frac{\int_0^1 d\lambda\int_0^{\lambda}d\lambda' C(\mathbf{r},\mathbf{r}';[\lambda'\rho_s])}{\int_0^1 d\lambda\int_0^{\lambda}d\lambda'\int d\mathbf{r}C(|\mathbf{r}|;\lambda'\hat{\rho}_1[\rho_s])}\ , \tag{3.4b}$$

which shows that $\hat{\rho}_1$, if it exists, must have the form of a doubly weighted solid density (3.4a) with $w(\mathbf{r},\mathbf{r}';[\rho_s])$ of (3.4b) as a weighting function. Notice that in the uniform

limit $\rho_s(\mathbf{r})\to\rho_l$, we have $C(\mathbf{r},\mathbf{r}';[\rho_s])\to C(|\mathbf{r}-\mathbf{r}'|;\rho_l)$ and (3.4b) implies then that $w(\mathbf{r},\mathbf{r}';[\rho_s])\to w(|\mathbf{r}-\mathbf{r}'|;\rho_l)$ with

$$\int d\mathbf{r}\, w(|\mathbf{r}|;\rho_l)=1 , \tag{3.5}$$

where we have already taken into account that (3.4a) implies that

$$\hat{\rho}_1[\rho_s]\to\rho_l \quad \text{when } \rho_s(\mathbf{r})\to\rho_l . \tag{3.6}$$

Notice also from (3.4b) that the normalization property (3.5) holds only in this uniform limit.

(ii) *Structural mapping.* One may also observe that the only unknown of (2.14) is, in fact, the DCF of the solid. It is thus possible to map, instead of the full $F_{ex}[\rho_s]$ expression, only the DCF of the solid onto that of some effective liquid. The attention is hereby shifted from a thermodynamic property (F_{ex}) to a structural property (the DCF). One obvious difference between the DCF of a solid and of a liquid is that the latter is a translationally invariant function while the former is not. This difficulty can be easily bypassed by observing that the only thing which matters for the computation of $F_{ex}[\rho_s]$, which is our final goal, is the density averaged DCF [cf. Eq. (2.14)]. The structural mapping of the solid onto the effective liquid can thus be defined by

$$\int d\mathbf{r}\int d\mathbf{r}'\rho_s(\mathbf{r})\rho_s(\mathbf{r}')C(\mathbf{r},\mathbf{r}';[\rho_s]) = \int d\mathbf{r}\int d\mathbf{r}'\rho_s(\mathbf{r})\rho_s(\mathbf{r}')C(|\mathbf{r}-\mathbf{r}'|;\hat{\rho}_2) , \tag{3.7}$$

where $\hat{\rho}_2$ is the (uniform) density of the effective liquid whose DCF is used to describe the averaged DCF of the solid of density $\rho_s(\mathbf{r})$. According to the structural mapping of Eq. (3.7), we have

$$\hat{\rho}_2=\hat{\rho}_2[\rho_s] , \tag{3.8}$$

a relation which is the structural analog of (3.2). Equation (3.7) implies then that Eq. (2.14) can be rewritten as

$$\beta F_{ex}[\rho_s]=-\int d\mathbf{r}\int d\mathbf{r}'\int_0^1 d\lambda\int_0^\lambda d\lambda'\rho_s(\mathbf{r})\rho_s(\mathbf{r}') \times C(|\mathbf{r}-\mathbf{r}'|;\hat{\rho}_2[\lambda'\rho_s]) , \tag{3.9}$$

which when compared to Eq. (2.16) shows that in the uniform limit $\rho_s(\mathbf{r})\to\rho_l$ we must have $\hat{\rho}_2[\rho_s]\to\rho_l$, just as for the thermodynamic mapping [cf. (3.6)].

Notice, finally, that if we combine the thermodynamic mapping of (3.3) and the structural mapping of (3.7), we obtain instead of (3.4), the expression

$$\hat{\rho}_1[\rho_s]=\frac{\int d\mathbf{r}\int d\mathbf{r}'\rho_s(\mathbf{r})\rho_s(\mathbf{r}')\int_0^1 d\lambda\int_0^\lambda d\lambda' C(|\mathbf{r}-\mathbf{r}'|;\hat{\rho}_2[\lambda'\rho_s])}{\rho_s V\int_0^1 d\lambda\int_0^\lambda d\lambda'\int d\mathbf{r}C(|\mathbf{r}|;\lambda'\hat{\rho}_1[\rho_s])} , \tag{3.10}$$

which is now entirely expressed in terms of the liquid DCF.

This is as far as one can go (on general grounds) with the idea of mapping the thermodynamic properties (here F_{ex}) of a nonuniform system (here the solid) onto the (thermodynamic or structural) properties of a uniform system (here the liquid). If these mappings exist and are unique, then the above relations will remain exact. We now consider some of the approximate determinations of these mappings.

A. Generalized effective liquid approximation (GELA)

The above ideas are useful only if they lead to some practical way of computing the excess free energy of the solid. Given some liquid DCF and $\rho_s(\mathbf{r})$ (which will be determined later by minimizing the *total* free energy) we have to determine both $\hat{\rho}_1[\rho_s]$ and $\hat{\rho}_2[\rho_s]$ in order to find $F_{ex}[\rho_s]$ from Eq. (3.10). The basic assumption which will be made here is that the effective liquid which is used to reproduce the (density averaged) structure of the solid should also reproduce its thermodynamics (here the excess free energy per particle), i.e., we identify the thermodynamic and the structural mapping as being one and the same mapping, or explicitly,

$$\hat{\rho}_1[\rho_s]=\hat{\rho}_2[\rho_s]\equiv\hat{\rho}[\rho_s] , \tag{3.11}$$

This can also be rephrased by saying that the thermodynamic mapping *defines* what we mean by "effective liquid" while the structural mapping is the unique approximation used to *close* the equations.

In this case $\hat{\rho}[\rho_s]$ will be defined by Eq. (3.10), which becomes now using (3.11)

$$\hat{\rho}[\rho_s]=\frac{\int d\mathbf{r}\int d\mathbf{r}'\rho_s(\mathbf{r})\rho_s(\mathbf{r}')\int_0^1 d\lambda\int_0^\lambda d\lambda' C(|\mathbf{r}-\mathbf{r}'|;\hat{\rho}[\lambda'\rho_s])}{\rho_s V\int_0^1 d\lambda\int_0^\lambda d\lambda'\int d\mathbf{r}C(|\mathbf{r}|;\lambda'\hat{\rho}[\rho_s])} , \tag{3.12}$$

which has the appearance of a self-consistent equation for the determination of $\hat{\rho}$ in terms of $\rho_s(\mathbf{r})$ and the liquid DCF $C(|\mathbf{r}|;\rho_l)$. The self-consistent aspect of Eq. (3.12) is due to the fact that we have imposed a self consistency between the structure and the thermodynamics of the *effective* liquid. In order to avoid confusion with some of the earlier approxi-

mation schemes,[6,9] we will call the present approximation (3.12) the "generalized" effective liquid approximation.[10] Changing $\rho_s(\mathbf{r})$ to $\lambda\rho_s(\mathbf{r})$ in Eq. (3.12) we obtain a more convenient form for this integral equation:

$$\hat{\rho}[\lambda\rho_s]=\frac{\int d\mathbf{r}\int d\mathbf{r}'\rho_s(\mathbf{r})\rho_s(\mathbf{r}')\frac{1}{\lambda}\int_0^{\lambda}d\alpha\int_0^{\alpha}d\alpha' C(|\mathbf{r}-\mathbf{r}'|;\hat{\rho}[\alpha'\rho_s])}{\rho_s V\int_0^1 d\alpha\int_0^{\alpha}d\alpha'\int d\mathbf{r}C(|\mathbf{r}|;\alpha'\hat{\rho}[\lambda\rho_s])}\ , \tag{3.13}$$

which is equivalent to the following differential equation:

$$\frac{\partial^2}{\partial\lambda^2}(\lambda\beta\phi_{\rm ex}(\hat{\rho}[\lambda\rho_s]))=-\frac{1}{\rho_s V}\int d\mathbf{r}\int d\mathbf{r}'\rho_s(\mathbf{r})\rho_s(\mathbf{r}')C(|\mathbf{r}-\mathbf{r}'|;\hat{\rho}[\lambda\rho_s])\ , \tag{3.14}$$

where $\phi_{\rm ex}(\hat{\rho})$ is the excess free energy per particle of the liquid as obtained from Eq. (2.16). Once Eq. (3.14), or Eq. (3.12), has been solved for $\hat{\rho}[\rho_s]$ we obtain the excess free energy of the solid from either (3.1) (with $\hat{\rho}_1[\rho_s]\equiv\hat{\rho}[\rho_s]$) or from (3.9) (with $\hat{\rho}_2[\rho_s]\equiv\hat{\rho}[\rho_s]$):

$$\beta F_{\rm ex}^{\rm GELA}[\rho_s]=-\rho_s V\hat{\rho}[\rho_s]\int_0^1 d\lambda\int_0^{\lambda}d\lambda'\int d\mathbf{r}C(|\mathbf{r}|;\lambda'\hat{\rho}[\rho_s]) \tag{3.15a}$$

$$=-\int d\mathbf{r}\int d\mathbf{r}'\int_0^1 d\lambda\int_0^{\lambda}d\lambda'\rho_s(\mathbf{r}')\rho_s(\mathbf{r})C(|\mathbf{r}-\mathbf{r}'|;\hat{\rho}[\lambda'\rho_s])\ . \tag{3.15b}$$

Notice also that $\hat{\rho}$ of Eq. (3.12) can be written, in analogy with (3.4), as a doubly weighted density:

$$\hat{\rho}[\rho_s]=\frac{1}{\rho_s V}\int d\mathbf{r}\int d\mathbf{r}'\rho_s(\mathbf{r})\rho_s(\mathbf{r}')\times w^{\rm GELA}(|\mathbf{r}-\mathbf{r}'|;[\rho_s])\ , \tag{3.16a}$$

$$W^{\rm GELA}(|\mathbf{r}-\mathbf{r}'|;[\rho_s])=\frac{\int_0^1 d\lambda\int_0^{\lambda}d\lambda' C(|\mathbf{r}-\mathbf{r}'|;\hat{\rho}[\lambda'\rho_s])}{\int_0^1 d\lambda\int_0^{\lambda}d\lambda'\int d\mathbf{r}C(|\mathbf{r}|;\lambda'\hat{\rho}[\rho_s])}\ , \tag{3.16b}$$

where it should be observed that the weighting function is normalized only in the uniform limit [cf. (3.5)]. The major interest of the GELA, defined by say Eqs. (3.12) and (3.15a), is that it maintains all the formal properties of the exact $F_{\rm ex}[\rho_s]$ [cf. Eq. (2.9)]. This is due to the fact that Eq. (3.15b) establishes the same functional relation between $F_{\rm ex}^{\rm GELA}[\rho_s]$ and $C(|\mathbf{r}-\mathbf{r}'|;\hat{\rho}[\rho_s])$ as does Eq. (2.14) for the exact $F_{\rm ex}[\rho_s]$ and $C(\mathbf{r},\mathbf{r}';[\rho_s])$. As a consequence we obtain from (3.15b) that

$$\frac{\delta\beta F_{\rm ex}^{\rm GELA}[\rho_s]}{\delta\rho_s(\mathbf{r})}=-\int d\mathbf{r}'\int_0^1 d\lambda\,\rho_s(\mathbf{r}')C(|\mathbf{r}-\mathbf{r}'|;\hat{\rho}[\lambda\rho_s])\ , \tag{3.17}$$

$$\frac{\delta^2\beta F_{\rm ex}^{\rm GELA}[\rho_s]}{\delta\rho_s(\mathbf{r})\delta\rho_s(\mathbf{r}')}=-C(|\mathbf{r}-\mathbf{r}';\hat{\rho}[\rho_s])\ , \tag{3.18}$$

$$\frac{\delta^n\beta F_{\rm ex}^{\rm GELA}[\rho_s]}{\delta\rho_s(\mathbf{r}_1)\cdots\delta\rho_s(\mathbf{r}_n)}=-\frac{\delta^{n-2}C(|\mathbf{r}_1-\mathbf{r}_2|;\hat{\rho}[\rho_s])}{\delta\rho_s(\mathbf{r}_2)\cdots\delta\rho_s(\mathbf{r}_n)}\ , \tag{3.19}$$

which correspond to the formal properties (2.9). [Notice that for $n>2$ the right-hand side (rhs) of Eq. (3.19) has to be symmetrized with respect to the arguments $\mathbf{r}_1,\ldots,\mathbf{r}_n$.] The GELA thus expresses the excess thermodynamic properties of the solid in terms of the DCF of the liquid, maintains all the formal properties of the DF theory and remains exact in the uniform limit. This is about as far as one can possibly go with the effective liquid idea. Notice that in the uniform limit Eq. (3.19) can also be used to study the higher-order DCF of the *liquid*.[11] Because of the translational invariance of the rhs of (3.18) it can, however, not be used to study the structural properties of the solid (remember however that it is the *thermodynamic* properties of the solid we originally set out to study here). Finally, we note that the major asset of the property expressed in Eq. (3.18) is that the GELA is a complete theory. If Eq. (3.18) did not hold, then the approximate free-energy functional we obtained would imply some new effective liquid DCF. One would then be forced to solve Eqs. (3.16) again with this new DCF, and to thus iterate until Eq. (3.18) was satisfied, if one wished to obtain a self-consistent solution. This is, in fact, the case with all the other nonperturbative DF theories, although, because of its difficulty, no one did actually carry out this iteration process.

B. The self-consistent effective liquid approximation (SCELA)

In an earlier publication[9] one of us introduced an approximation closely related to the GELA but which was based on a slightly different structural mapping. This approximation, which was called the self-consistent effective liquid approximation (notice, however, that the GELA is in fact more "self consistent" than the SCELA), is based on the same thermodynamic mapping as that of Eq. (3.15a) but replaces the structural mapping of (3.15b) by

$$\beta F_{\rm ex}^{\rm SCELA}[\rho_s]=-\int d\mathbf{r}\int d\mathbf{r}'\int_0^1 d\lambda\int_0^{\lambda}d\lambda'\rho_s(\mathbf{r})\rho_s(\mathbf{r}')\times C(|\mathbf{r}-\mathbf{r}'|;\lambda'\hat{\rho}[\rho_s])\ , \tag{3.20}$$

which differs from (3.15b) in that $\hat{\rho}[\lambda\rho_s]$ has been replaced by $\lambda\hat{\rho}[\rho_s]$ in the density argument of the liquid

DCF. This then has the technical advantage that the basic integral equation (3.12) is transformed into a transcendental equation involving only $\hat{\rho}[\rho_s]$, whereas (3.12) involves both $\hat{\rho}[\rho_s]$ and $\hat{\rho}[\lambda\rho_s]$. An important physical consequence of this, however, is that the structural relations (3.18) and (3.19) are lost. In the SCELA equations (3.16a) and (3.16b) become

$$\hat{\rho}[\rho_s]=\frac{1}{\rho_s V}\int d\mathbf{r}\int d\mathbf{r}'\rho_s(\mathbf{r})\rho_s(\mathbf{r}')w^{\mathrm{SCELA}}(|\mathbf{r}-\mathbf{r}'|;[\rho_s]) , \tag{3.21a}$$

$$w^{\mathrm{SCELA}}(|\mathbf{r}-\mathbf{r}'|;[\rho_s]) = \frac{\int_0^1 d\lambda\int_0^\lambda d\lambda' C(|\mathbf{r}-\mathbf{r}'|;\lambda\hat{\rho}[\rho_s])}{\int_0^1 d\lambda\int_0^\lambda d\lambda'\int d\mathbf{r}\, C(|\mathbf{r}|;\lambda'\hat{\rho}[\rho_s])} , \tag{3.21b}$$

so that one now has the normalization property

$$\int d\mathbf{r}\, w^{\mathrm{SCELA}}(|\mathbf{r}|;[\rho_s])=1 \tag{3.22}$$

satisfied for any $\rho_s(\mathbf{r})$. The SCELA is exact in the uniform limit (just as is the GELA) because both $\hat{\rho}[\lambda\rho_s]$ and $\lambda\hat{\rho}[\rho_s]$ tend to $\lambda\rho_l$ when $\rho_s(\mathbf{r})$ tends to ρ_l. Besides this the SCELA can be considered as a further approximation to the GELA. We have found (see below) that in fact the SCELA yields a rather good approximation to the GELA. This can be understood by observing that in the end points of the λ integrals appearing in (3.21b), i.e., for $\lambda=0$ and $\lambda=1$ [see (2.12)], $\hat{\rho}[\lambda\rho_s]$ and $\lambda\hat{\rho}[\rho_s]$ become identical.

C. The modified weighted-density approximation (MWDA)

Recently, Denton and Ashcroft[12] have introduced a nonperturbative approximate DF theory which they called the modified weighted-density approximation (MWDA) because it is based on some of the ideas of the weighted-density approximation (WDA) of Curtin and Ashcroft,[13] which is itself a nonperturbative generalization of the earlier theory of Tarazona.[14] The latter two theories[13,14] are intrinsically more complicated theories than those considered here because they involve a *nonuniform* effective liquid and require consideration of the *local* excess free energy, $\psi_{\mathrm{ex}}(\mathbf{r};[\rho_s])$ of Eq. (2.4). We will therefore not consider these theories here although they could be discussed along similar lines as already explained elsewhere.[9]

We now return to the MWDA of Denton and Ashcroft.[12] This theory is based on the thermodynamic mapping (3.1):

$$\phi_{\mathrm{ex}}^{\mathrm{MWDA}}[\rho_s]=\phi_{\mathrm{ex}}(\hat{\rho}) , \tag{3.23}$$

but contrary to (3.1) the DF expression (2.14) for $\phi_{\mathrm{ex}}[\rho_s]$ is not used, so that (3.4) does not follow here. Instead, (3.4a) is *postulated:*

$$\hat{\rho}[\rho_s]=\frac{1}{\rho_s V}\int d\mathbf{r}\int d\mathbf{r}'\rho_s(\mathbf{r})\rho_s(\mathbf{r}') \times w^{\mathrm{MWDA}}(|\mathbf{r}-\mathbf{r}'|;[\rho_s]) , \tag{3.24}$$

where the weighting function $w^{\mathrm{MWDA}}(|\mathbf{r}|;[\rho_s])$ is not given directly by (3.4b) but is *defined* by requiring that (i) it be normalized

$$\int d\mathbf{r}\, w^{\mathrm{MWDA}}(|\mathbf{r}|;[\rho_s])=1 , \tag{3.25}$$

and (ii) it be a function of $\hat{\rho}[\rho_s]$

$$w^{\mathrm{MWDA}}(|\mathbf{r}|;[\rho_s])=w^{\mathrm{MWDA}}(|\mathbf{r}|;\hat{\rho}[\rho_s]) , \tag{3.26}$$

so that Eq. (3.24) becomes a self-consistency relation, and (iii) that it be further determined implicitly by requiring the following relation:

$$\left.\frac{\delta^2\beta F_{\mathrm{ex}}^{\mathrm{MWDA}}[\rho_s]}{\delta\rho_s(\mathbf{r})\delta\rho_s(\mathbf{r}')}\right|_{\rho_s(\mathbf{r})=\rho_l} = -C(|\mathbf{r}-\mathbf{r}'|;\rho_l) \tag{3.27}$$

to hold for any uniform density ρ_l. The result they obtain is that

$$w^{\mathrm{MWDA}}(|\mathbf{r}|;\rho_l)=\frac{(C|\mathbf{r}|;\rho_l)+\frac{1}{V}\rho_l\beta\phi_{\mathrm{ex}}''(\rho_l)}{\int d\mathbf{r}\left[C(|\mathbf{r}|;\rho_l)+\frac{1}{V}\rho_l\beta\phi_{\mathrm{ex}}''(\rho_l)\right]} , \tag{3.28}$$

where $\phi_{\mathrm{ex}}''(\rho_l)=\partial^2\phi_{\mathrm{ex}}(\rho_l)/\partial\rho_l^2$, with $\phi_{\mathrm{ex}}(\rho_l)$ the excess free-energy per particle of the liquid [cf. Eq. (2.16)]. Notice the following relations (i) Equations (3.23) and (3.24) are identical to those of the GELA or the SCELA, except for the fact that here Eq. (3.24) is postulated whereas in the former theories it is derived from Eq. (3.23). (ii) Equations (3.25) and (3.26) are valid in the SCELA but not in the GELA. (iii) Equation (3.27) holds only in the GELA [where the stronger property (3.18) holds] but not in the SCELA. Notice finally that both in the GELA and in the SCELA, the weighting function [see (3.16) and (3.21)] has the same range as the liquid DCF whereas here it has an infinite range [see (3.28)]. From the present DF viewpoint it also appears that the normalization condition (3.25) and (3.26) of the MWDA is in fact incompatible with the requirement of (3.27), as can be seen from the fact that in (3.4b) the exact weighting function cannot be normalized.

D. The effective liquid approximation (ELA)

In the earlier theory of Baus and Colot[6] Eq. (2.19) was taken as starting point. Although this relation is as exact as (2.14), the fact that it uses a liquid as reference state for the functional integration of (2.13) [see (2.10)] precludes a direct comparison with the above approximation schemes. For the sake of completeness, it is nevertheless of interest to rephrase the original effective liquid approximation[6] in the present language. Only the structural mapping (3.7) was used in this theory, so that Eq. (2.18) becomes

$$\beta F_{ex}[\rho_s]=\beta F_{ex}(\rho_l)+\beta V(\rho_s-\rho_l)\mu_{ex}(\rho_l) - \int d\mathbf{r}\int d\mathbf{r}\int_0^1 d\lambda(1-\lambda) \times C(|\mathbf{r}-\mathbf{r}'|;\hat{\rho}_2[\rho_l+\lambda(\rho_s-\rho_l)]) \times(\rho_s(\mathbf{r})-\rho_l)(\rho_s(\mathbf{r}')-\rho_l) . \quad (3.29)$$

Furthermore, the structural relation (3.8) $\hat{\rho}_2=\hat{\rho}_2[\rho_s]$ was taken not from DF theory but from an extraneous condition relating the density of the effective liquid $\hat{\rho}_2$ to the position of the shortest nonzero reciprocal-lattice vector (RLV) of the solid by scaling the position of the main peak of the static structure factor of the effective liquid to this RLV. Since this RLV depends only on the average density ρ_s of the solid [see (2.1)], the functional $\hat{\rho}_2[\rho_s]$ degenerates in this case into an ordinary function $\hat{\rho}_2(\rho_s)$. The density argument of the DCF of (3.29) then becomes $\hat{\rho}_2[\rho_l+\lambda(\rho_s-\rho_l)]$, which by a particular choice of the reference state ρ_l, namely $\rho_l=\rho_s$, can moreover be made independent of λ. For this particular reference state the second term in the rhs of Eq. (3.29) also drops out and one obtains finally:

$$\beta F_{ex}^{ELA}[\rho_s]=\beta F_{ex}(\rho_s)-\frac{1}{2}\int d\mathbf{r}\int d\mathbf{r}' C[|\mathbf{r}-\mathbf{r}'|;\hat{\rho}_2(\rho_s)] \times(\rho_s(\mathbf{r})-\rho_s) \times(\rho_s(\mathbf{r}')-\rho_s) , \quad (3.30)$$

where the λ integral has been trivially performed [$\int_0^1 d\lambda(1-\lambda)=\frac{1}{2}$]. The somewhat surprising result is that although this theory uses no expansions and hence is nonperturbative, the final equation (3.30) is quite similar to the second-order approximation of Ramakrishnan and Yussouff[8] [compare Eqs. (3.30) and (2.20)]. This has led to some confusion in the literature. The clue to Eq. (3.30) is that a very simple structural mapping $\hat{\rho}_2[\rho_s]\equiv\hat{\rho}_2(\rho_s)$ has been used. An important limitation of this mapping however is that it is tightly bound to crystalline solids whereas the present theories, such as the GELA, are completely general and can, in principle, be applied to any nonuniform system.

E. Relation between the GELA, SCELA, and MWDA

From the above it should be clear that from all the nonperturbative DF theories, the GELA, SCELA, and MWDA appear to be more closely related than the ELA and the WDA which have a somewhat different status. In what follows we point out the exact relation between the GELA, SCELA, and MWDA. Let us start from the more general GELA. As we have seen this theory results from the introduction of a *single* approximation (the structural mapping) into the exact (thermodynamic) mapping between the solid and the liquid excess thermodynamics. Both the SCELA and the MWDA introduce additional assumptions. Here we will show that both these theories can be viewed as *mathematically* well defined approximations to the solution of the GELA. To do so we solve the GELA by expanding $\hat{\rho}[\lambda\rho_s]$ around $\lambda=1$, since $\hat{\rho}[\rho_s]$ is the only quantity which matters for evaluating the excess free energy of the solid according to Eq. (3.1). Equations (3.13) and (3.14) suggest then that this expansion can be written as

$$\hat{\rho}[\lambda\rho_s]=\lambda\left[\sum_{n=0}^{\infty}(\lambda-1)^n a_n[\rho_s]\right] \quad (3.31)$$

with $\hat{\rho}[\rho_s]\equiv a_0[\rho_s]$. Substituting the expansion (3.31) into Eq. (3.13) and differentiating with respect to λ yields a sequence of equations which, when λ is set equal to 1, can serve to determine the $\{a_n\}$ of (3.31). The first few equations so obtained read

$$\beta\phi_{ex}(a_0)=-\frac{1}{\rho_s V}\int d\mathbf{r}\int d\mathbf{r}'\rho_s(\mathbf{r})\rho_s(\mathbf{r}')\int_0^1 d\alpha\int_0^\alpha d\alpha' C(|\mathbf{r}-\mathbf{r}'|;\hat{\rho}[\alpha'\rho_s]) , \quad (3.32a)$$

$$\beta\phi_{ex}(a_0)+(a_0+a_1)\beta\phi'_{ex}(a_0)=-\frac{1}{\rho_s V}\int d\mathbf{r}\int d\mathbf{r}'\rho_s(\mathbf{r})\rho_s(\mathbf{r}')\int_0^1 d\alpha C(|\mathbf{r}-(\mathbf{r}')|;\hat{\rho}[\alpha\rho_s]) , \quad (3.32b)$$

$$2(a_0+2a_1+a_2)\beta\phi'_{ex}(a_0)+(a_0+a_1)^2\beta\phi''_{ex}(a_0)=-\frac{1}{\rho_s V}\int d\mathbf{r}\int d\mathbf{r}'\rho_s(\mathbf{r})\rho_s(\mathbf{r}')C(|\mathbf{r}-\mathbf{r}'|;\hat{\rho}[\rho_s]) , \quad (3.32c)$$

etc., where $a_n\equiv a_n[\rho_s]$,

$$\phi'_{ex}(\rho)=\frac{\partial\phi_{ex}(\rho)}{\partial\rho}, \quad \phi''_{ex}(\rho)=\frac{\partial^2\phi_{ex}(\rho)}{\partial\rho^2} ,$$

and $\hat{\rho}[\alpha\rho_s]$ in the rhs of (3.32) is meant to be expressed by (3.31). Notice also that Eqs. (3.32a) and (3.32b) involve all the coefficients $\{a_n\}$ while the remaining equations relate only a finite number of them [the first three for Eq. (3.32c)]. To solve the GELA one can then determine the $\{a_n\}$ by successive approximation. First we set $a_n\equiv 0$ for $n>0$ and determine a_0 from (3.32a). Notice that this first-order GELA solution is nothing but the solution of the SCELA for which one has indeed that $\hat{\rho}[\lambda\rho_s]=\lambda a_0[\rho_s]\equiv\lambda\hat{\rho}[\hat{\rho}_s]$. Next we keep only a_0 and a_1 in (3.31) and determine these from (3.32a) and (3.32b) leading to the second-order GELA solution. Continuing this process but remembering that what we need to determine the excess free energy of the solid is only $a_0[\rho_s]\equiv\hat{\rho}[\rho_s]$, we may terminate the sequence of approximations when the change in a_0 becomes sufficiently small (generally, the third-order solution is sufficient, see

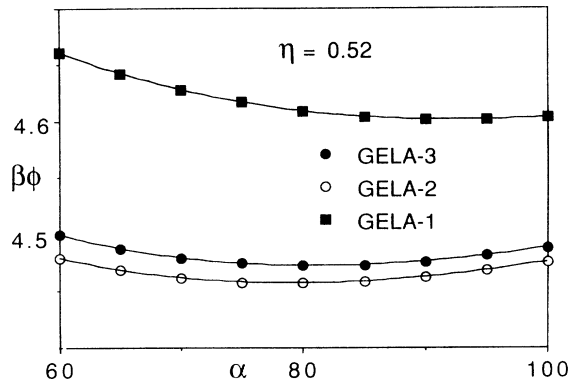

FIG. 1. As an illustration of the convergence of the iterative solution of the GELA obtained from the procedure described in Sec. III E, we show an enlarged view of the reduced free energy per particle ($\beta\phi$), in the region of the minimum, vs the Gaussian width order parameter ($\alpha\sigma^2$) for a HS solid of packing fraction $\eta=0.52$ as obtained in first, second, and third order. Notice that the first-order solution (GELA-1) is identical to the SCELA. The change from first- to second-order solution is appreciable but when going from the second- to the third-order solution the position of the minimum remains stable while the relative change in $\beta\phi$ is 2.10^{-3}.

Fig. 1). We thus find that although the GELA is defined by a complicated integral equation, its implementation actually involves little more computational effort than the simpler SCELA, which corresponds to the first-order GELA. Similarly, the MWDA solution results if we *disregard* Eqs. (3.32a) and (3.32b) and solve Eq. (3.32c) with the additional constraints $a_1=(\rho_s a_0)^{1/2}-a_0$ and $a_2=-2a_1$ so that $a_0\equiv\hat{\rho}[\rho_s]$ is the only unknown. Thus, notwithstanding its physically very different derivation, the additional physical assumptions of the MWDA, just as the SCELA, can be recast as a mathematical approximation to the equations (3.31) and (3.32) defining the solution of the more general GELA theory.

IV. APPLICATION TO THE HARD-SPHERE (HS) SOLID

We now will compare the theoretical predictions of these different nonperturbative DF theories for the particular case of the hard-sphere solid.[10] This does not imply that these theories are in any sense restricted to the HS system but simply that, because of its relative simplicity, this system provides a convenient testing ground. Since the results of the ELA (Refs. 6 and 15) and the MWDA (Ref. 12) for the HS system have already been discussed in detail elsewhere we will focus here mainly on the predictions of the GELA and the SCELA. Our purpose will thus be the explicit computation of the free-energy per particle ϕ of the HS system. This naturally splits into the computation of the ideal part $\phi_{\rm id}$ and the excess part $\phi_{\rm ex}$ of the total free energy $\phi=\phi_{\rm id}+\phi_{\rm ex}$. Knowing ϕ we can obtain the pressure p and the chemical potential μ from the well-known[4] thermodynamic relations

$$p=\rho^2\frac{\partial\phi}{\partial\rho},\quad \mu=\frac{\partial}{\partial\rho}(\rho\phi)\ , \tag{4.1}$$

where ρ is the average number density [cf. Eq. (2.1)].

For the HS *fluid* these quantities are known from various theories:[4]

$$\beta\phi=(\ln\Lambda^3\rho-1)+(\gamma-1)\left[\ln(1-\eta)+\eta\frac{\left[1-\frac{3}{2}\eta\right]}{(1-\eta)^2}\right]+\eta\frac{(4-3\eta)}{(1-\eta)^2}$$
$$\equiv(\ln\Lambda^3\rho-1)+\beta\phi_{\rm ex}\ , \tag{4.2}$$

$$\frac{\beta p}{\rho}=\frac{1+\eta+\eta^2-\gamma\eta^3}{(1-\eta)^3}\ , \tag{4.3}$$

$$\beta\mu=\frac{\beta p}{\rho}+\beta\phi\ , \tag{4.4}$$

where $\eta=(\pi/6)\sigma^3\rho$ is the packing fraction of HS of diameter σ. In Eqs. (4.2)–(4.4) the parameter γ has been introduced in order to distinguish the different theoretical results for the fluid phase:[4] $\gamma=0$ for the Percus-Yevick (PY) compressibility results, $\gamma=3$ for the PY virial results, and $\gamma=1$ for the Carnahan-Starling (CS) results. The latter results (CS) are virtually identical to the computer simulation results of the HS fluid phase. This information will now be used to construct the free energy of the HS *solid*.

A. The ideal free energy

The ideal part of the free energy per particle of the solid reads

$$\beta\phi_{\rm id}[\rho_s]=\frac{1}{\rho_s V}\int d\mathbf{r}\,\rho_s(\mathbf{r})\{\ln[\Lambda^3\rho_s(\mathbf{r})]-1\}\ , \tag{4.5}$$

where $\rho_s(\mathbf{r})$ is the periodic density of the bulk solid. Normally the symmetry breaking features of $\rho_s(\mathbf{r})$ should be fixed by (i) introducing a symmetry-breaking external field [see (2.3)], (ii) taking the thermodynamic limit of a large system, and (iii) letting the amplitude of the external field vanish. Here we will, as usual,[3] introduce the symmetry breaking "by hand" and omit all together the external field from our considerations. We thus write, using a Gaussian approximation for the density profiles,

$$\rho_s(\mathbf{r})=\sum_i\left[\frac{\alpha}{\pi}\right]^{3/2}\exp-\alpha(\mathbf{r}-\mathbf{R}_i)^2\ , \tag{4.6a}$$

$$\rho_s(\mathbf{r})=\rho_s\sum_j\exp(-\mathbf{k}_j^2/4\alpha)\exp(i\mathbf{k}_j\cdot\mathbf{r})\ , \tag{4.6b}$$

where $\{\mathbf{R}_i\}$ are the Bravais lattice vectors of the crystal structure and $\{\mathbf{k}_j\}$ the corresponding reciprocal lattice vectors. The Gaussian approximation embodied in (4.6) is not exact since the density peaks are usually slightly anisotropic. It is however a very good first approximation[15] which has moreover the great advantage that the solid density can be described in terms of a single order parameter α the inverse width of the Gaussians. For

$\alpha>0$ Eq. (4.6) describes a periodic solidlike density while for $\alpha=0$ it yields a uniform fluidlike density. The value of α describing the actual solid will be determined later by minimizing the *total* free energy with respect to α. The lattice structure used in (4.6) could in principle be sorted out by the theory[16] but this leads to quite cumbersome expressions. In practice it is much easier to repeat the free-energy evaluation for a few physically plausible structures and determine the absolute free-energy minimum by comparing the different calculations. Here we will perform such calculations for the cubic lattices (fcc, bcc, and sc). Although it is known that fcc (or any other compact structure[15]), is the equilibrium structure, this procedure will allow us to extract some interesting information about the metastable HS solids (here bcc and sc). Anticipating our results, we will find that in the equilibrium solid (fcc) the particles are well localized, corresponding to large α values. In this case it is more convenient to use the real-space representation (4.6a). In the metastable solids (bcc, sc) the particles will instead be much more delocalized, corresponding to much smaller α values. In this case it is often easier to use the reciprocal-space representation (4.6b). If we want to study both the stable and metastable solid structures it will thus be necessary to evaluate (4.5) both for small and large α values. Consider first the large α values. Using (4.6a) in (4.5) one obtains, using moreover the periodicity of the lattice,

$$\begin{aligned}\beta\phi_{\rm id}&=\ln\left[\frac{\Lambda}{\sigma}\right]^3-1+\left[\frac{\alpha}{\pi}\right]^{3/2}\int d\mathbf{r}\exp(-\alpha\mathbf{r}^2)\ln[\sigma^3\rho_s(\mathbf{r})]\\&=\ln\left[\frac{\Lambda}{\sigma}\right]^3-1+\left[\frac{\alpha}{\pi}\right]^{3/2}\int d\mathbf{r}\exp(-\alpha\mathbf{r}^2)\ln\left[\left[\frac{\alpha\sigma^2}{\pi}\right]^{3/2}\exp(-\alpha\mathbf{r}^2)\left[1+{\sum_i}'e^{[-\alpha(\mathbf{r}-\mathbf{R}_i)^2-\alpha\mathbf{r}^2]}\right]\right]\\&=\ln\left[\frac{\Lambda}{\sigma}\right]^3-\frac{5}{2}+\ln\left[\frac{\alpha\sigma^2}{\pi}\right]^{3/2}+\frac{1}{\pi^{3/2}}\int d\mathbf{x}\,e^{-\mathbf{x}^2}\ln\left[1+{\sum_i}'e^{-[(\mathbf{x}-\sqrt{\alpha}\mathbf{R}_i)^2-\mathbf{x}^2]}\right],\end{aligned}\tag{4.7}$$

where $\mathbf{x}=\sqrt{\alpha}\mathbf{r}$, and the dash indicates that $\mathbf{R}_i\equiv0$ is excluded from the sum over $\{\mathbf{R}_i\}$. For large α values this sum is exponentially small and, to dominant order, Eq. (4.7) reduces simply to

$$\beta\phi_{\rm id}=\ln\left[\frac{\Lambda}{\sigma}\right]^3-\frac{5}{2}+\frac{3}{2}\ln\frac{\alpha\sigma^2}{\pi}\quad(\alpha\sigma^2\to\infty)\,.\tag{4.8}$$

By direct numerical integration it has been verified[6] that for the cubic lattices Eq. (4.8) can be used, with an accuracy of one part in 10^5, for $\alpha a^2\geq100$, where a is the lattice spacing. From Eq. (4.8) it is seen that $\phi_{\rm id}$ is a monotonically increasing function of α and hence that this term alone cannot stabilize the solid. For small α values we rewrite Eq. (4.7), using (4.6b) as

$$\begin{aligned}\beta\phi_{\rm id}&=\ln\left[\frac{\Lambda}{\sigma}\right]^3-1+\ln\rho_s\sigma^3+\frac{1}{\pi^{3/2}}\int d\mathbf{x}\,e^{-\mathbf{x}^2}\sum_{n=1}^{\infty}\frac{(-)^{n+1}}{n}\left[\frac{\rho_s(\mathbf{r})-\rho_s}{\rho_s}\right]^n\\&=\ln\left[\frac{\Lambda}{\sigma}\right]^3-1+\ln(\rho_s\sigma^3)+\sum_{n=1}^{\infty}\frac{(-)^{n+1}}{n}\int d\mathbf{x}\frac{1}{\pi^{3/2}}e^{-\mathbf{x}^2}\left[{\sum_j}'e^{-\mathbf{k}_j^2/4\alpha}e^{i\mathbf{k}_j\cdot\mathbf{r}}\right]^n\\&=\ln\left[\frac{\Lambda}{\sigma}\right]^3-1+\ln(\rho_s\sigma^3)+\sum_{n=1}^{\infty}\frac{(-)^{n+1}}{n}{\sum_{j_1,\ldots,j_n}}'e^{-(1/4\alpha)(\mathbf{k}_{j_1}^2+\cdots+\mathbf{k}_{j_n}^2)}e^{-(1/4\alpha)|\mathbf{k}_{j_1}+\cdots+\mathbf{k}_{j_n}|^2},\end{aligned}\tag{4.9}$$

where $\mathbf{x}=\sqrt{\alpha}\mathbf{r}$, and the dash indicates that $\mathbf{k}_j\equiv0$ is excluded from the sums over $\{\mathbf{k}_j\}$. For small α values, the dominant contributions come from the $n=1$ term with $\mathbf{k}_j=\mathbf{k}_1$ and from the $n=2$ term with $\mathbf{k}_j=\mathbf{k}_1$ and $\mathbf{k}_j,=-\mathbf{k}_1$, where $\mathbf{k}_1$ is the smallest nonzero RLV. To dominant order we obtain thus from (4.9) for small α values

$$\beta\phi_{\rm id}=\ln\left[\frac{\Lambda}{\sigma}\right]^3-1+\ln(\sigma^3\rho_s)+\tfrac{1}{2}C_1e^{-k_1^2/2\alpha},\quad\alpha\sigma^2\to0\tag{4.10}$$

where C_1 is the number of nearest neighbors in reciprocal space and $\mathbf{k}_1$ the shortest RLV. Unfortunately the asymptotic expansions of (4.8) and (4.10) do not match

very well for the intermediate α values. Therefore, we have used the numerical results of Baus and Colot[6] for $10 \leq \alpha a^2 \leq 100$, Eq. (4.8) for $\alpha a^2 \geq 100$, and Eq. (4.10) for $\alpha a^2 \leq 10$ [with C_1 in (4.10) slightly adjusted so as to match the numerical results[6] at $\alpha a^2 = 10$], where a is the lattice constant. In this way the accuracy of $\beta\phi_{\rm id}$ is estimated to be everywhere of one part in 10^5.

B. The excess free energy

For the nonperturbative DF theories under discussion here (essentially the GELA and the SCELA) the excess free energy per particle of the solid $\phi_{\rm ex}[\rho_s]$ is given in terms of the excess free energy per particle of the fluid $\phi_{\rm ex}(\rho_f)$ by

$$\phi_{\rm ex}[\rho_s] = \phi_{\rm ex}(\hat{\rho}) , \tag{4.11}$$

where $\hat{\rho}$ is the density of the effective fluid (or liquid) used to describe the solid [cf. Eq. (3.1)]. Once $\hat{\rho}$ is known $\phi_{\rm ex}(\hat{\rho})$ can be obtained from Eq. (2.17) by using the PY (HS) DCF or directly from the excess part of Eq. (4.2) (with $\gamma = 0$ for the PY DCF). Substituting this result in (4.11) we finally obtain the excess free energy $\phi_{\rm ex}$ of the solid. To determine $\hat{\rho}$ we return to (3.16) which we write using (4.6):

$$\hat{\rho} = \sum_i \left[\frac{\alpha}{2\pi} \right]^{1/2} \int_0^\infty dr \frac{r}{R_i} \left(e^{-(\alpha/2)(r-R_i)^2} - e^{(\alpha/2)(r+R_i)^2} \right) w(r;\hat{\rho}) , \tag{4.12a}$$

$$\hat{\rho} = \rho_s \sum_j e^{-k_j^2/2\alpha} \hat{w}(k_j;\hat{\rho}) \tag{4.12b}$$

where $r = |\mathbf{r}|$, $R_i \equiv |\mathbf{R}_i|$, $k_j = |\mathbf{k}_j|$, and $w(r;\hat{\rho})$ is the weighting function and $\hat{w}(k;\hat{\rho})$ its Fourier transform:

$$\hat{w}(k;\hat{\rho}) = \int d\mathbf{r}\, e^{i\mathbf{k}\cdot\mathbf{r}} w(r;\hat{\rho}) . \tag{4.13}$$

Here, in (4.12), and below we will take advantage of the fact that the functional form of $\rho_s(\mathbf{r})$ has been partially resolved by using (4.6) so that for a given lattice structure $\hat{\rho}$ becomes a function of α and of ρ_s, $\hat{\rho} = \hat{\rho}(\alpha, \rho_s)$, and we may thus drop henceforth the more accurate functional notation used in Secs. II and III. For $w(r;\hat{\rho})$ we obtain then using (3.16b), (2.12), and (2.16),

$$w(r;\hat{\rho}) = \frac{-\hat{\rho}}{\beta\phi_{\rm ex}(\hat{\rho})} \int_0^1 d\lambda (1-\lambda) C(r;\hat{\rho}(\lambda)) . \tag{4.14}$$

Because of the appearance of $\hat{\rho}(\lambda)$ in (4.14) it is in fact more convenient to start from (3.13) and rewrite Eqs. (4.12)–(4.14) in the form of an implicit equation for $\hat{\rho}(\lambda)$:

$$\beta\phi_{\rm ex}(\hat{\rho}(\lambda)) = -\sum_i \left[\frac{\alpha}{2\pi} \right]^{1/2} \int_0^\infty dr \frac{r}{R_i} \left(e^{-(\alpha/2)(r-R_i)^2} - e^{-\alpha_2(r+R_i)^2} \right) \int_0^\lambda d\lambda' \left[1 - \frac{\lambda'}{\lambda} \right] C(r;\hat{\rho}(\lambda')) , \tag{4.15a}$$

$$\beta\phi_{\rm ex}(\hat{\rho}(\lambda)) = -\rho_s \sum_j e^{-k_j^2/2\alpha} \int_0^\lambda d\lambda' \left[1 - \frac{\lambda'}{\lambda} \right] \hat{C}(k_j;\hat{\rho}(\lambda')) , \tag{4.15b}$$

where $\hat{C}(k;\hat{\rho})$ is the Fourier-transform of $C(r;\hat{\rho})$ defined as in (4.13). Using the results of Sec. III E, we can write $\hat{\rho}(\lambda)$ formally as in Eq. (3.31) and follow the procedure outlined there to solve (3.32) or (4.15) for the GELA solution.

Finally, to close the approximation, we will use as DCF for the effective fluid the PY result:[4]

$$C(r;\rho) = \Theta(1-x) \sum_{k=0,1,3} x^k C_k(\eta) \tag{4.16}$$

or one of its HS extensions.[17] In (4.16), $\Theta(x)$ is the Heaviside step function, $x = r/\sigma$, $C_0(\eta) \equiv -(1+2\eta)^2/(1-\eta)^4$, $C_1(\eta) \equiv 6\eta(1+\frac{1}{2}\eta)^2/(1-\eta)^4$, $C_3(\eta) \equiv (\eta/2)C_0(\eta)$, and $\eta = (\pi/6)\sigma^3\rho$ for HS of diameter σ and density ρ. Using (4.16) in (4.15) all the expressions can be computed analytically.[6,15] The solution of (4.15) will depend on the lattice structure (through $\{R_i\}$), on the lattice constant[15] or on ρ_s, and on α. To solve Eqs. (4.15) and (4.16) one can use the iterative procedure outlined in Sec. III E starting the search from $\hat{\rho} = \rho_s$. We have verified that changing this initial guess by an order of magnitude does not affect the results, indicating the uniqueness of the solution. For $\alpha a^2 \geq 30$ we have used (4.15a) while (4.15b) was used for $\alpha a^2 \leq 30$ with both results matching well at $\alpha a^2 \simeq 30$, a being the lattice constant. The iterative process converges very quickly; the influence of a_n with $n > 2$ in (3.31) on the result, $\hat{\rho} \equiv a_0$ was found to be small. A solution stable to one part in 10^5 can thus be easily obtained. This solution $\hat{\rho}$ is then used in (4.11) to obtain the excess free energy of the solid. Finally, the total free energy $\phi_{\rm id} + \phi_{\rm ex}$ is minimized with respect to α for each ρ_s and lattice structure. The resulting $\alpha_{\rm min}$ value, together with $\hat{\rho}(\alpha_{\rm min}(\rho_s), \rho_s)$ determines then the total free energy of the given crystal structure. The resulting free-energy data are then fitted to a fifth-order polynomial and the pressure p and chemical potential μ of the HS solid are finally obtained from this polynomial using Eq. (4.1).

C. The equilibrium HS solid

We have found that of all three cubic lattice structures, the fcc is the most stable one. In fact, instead of the fcc we could have used any compact structure (fcc, hcp, ran-

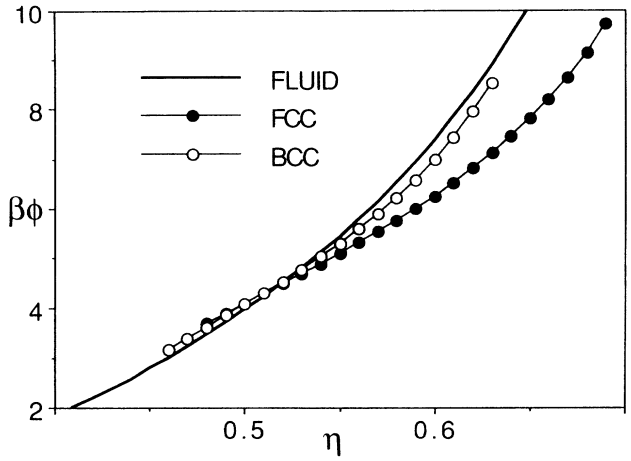

FIG. 2. The reduced free energy per particle ($\beta\phi$) vs the packing fraction (η) of the HS fluid, bcc, and fcc solid, as obtained from the GELA. The Carnahan-Starling approximation has been used for the actual fluid and the Percus-Yevick direct correlation function for the effective fluid describing the solid.

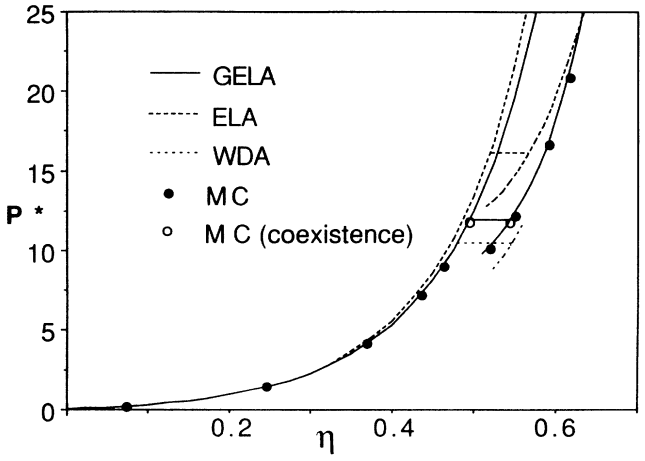

FIG. 3. The complete HS fluid-fcc phase diagram, in the pressure ($p^*=\beta p\sigma^3$)–density [$\eta=\rho\sigma^3(\pi/6)$] plane, as obtained from various nonperturbative density functional theories. Shown are the results of the GELA, the ELA (Ref. 6) and the WDA (Ref. 13) compared to the simulation results.[19–21] The tie lines separate the fluid and solid branches into a stable and metastable portion. On this scale the differences between the results of the SCELA and GELA and also between the MWDA and the WDA would not be visible (except for the position of the tie line which is given in Table I). All theories use the Percus-Yevick direct correlation function to describe the solid, and also for the fluid in the case of the ELA whereas the WDA and the GELA use the Carnahan-Starling approximation for the fluid.

dom compact stacking of dense lattice planes, etc.) without changing the results. This is due to the fact that the contribution to (4.15a) of the third neighbor shell, which could distinguish the compact structures, is negligible. The equilibrium HS solid is thus a compact structure. This is in agreement with the simulation results of Frenkel and Ladd.[18] Any differentiation between the compact structures would require a very precise determination of the tail of the HS DCF. The (fcc) HS solid is found to be stable up to the fcc close packing density ($\eta_{CP}=0.74$). Lowering the density an exchange of stability with respect to the HS fluid is found to occur at $\eta=0.515$ and finally below $\eta=0.480$ the fcc solid becomes unstable, i.e., the corresponding free-energy minimum disappears. This behavior is shown in Fig. 2. The pressure of the (stable and unstable) solid are compared to the simulation results[18] in Fig. 3. The agreement is very good. The results of the GELA and SCELA are very close one to another and both are superior to the other nonperturbative theories (MWDA, ELA, and also the WDA). To understand this excellent behavior we observe that the fcc HS solid is described here in terms of an effective HS fluid with a rather low density (see Fig. 4). In fact, for the stable solid these densities are low enough ($\eta \lesssim 0.4$) for the PY DCF (and its underlying PY compressibility equation of state) to become essentially exact. To test this we have repeated the calculations with an alternative HS DCF that contains the Carnahan-Starling equation of state[14] but this did not change the results. We also know[15] that for the compact fcc structure the Gaussian approximation for the density profiles is fairly accurate.[20] Therefore we may safely assume that one is testing here the basic assumptions behind the effective liquid idea of Sec. III and not its HS implementation. The possibility to map the thermodynamic properties of the HS solid onto those of an effective HS fluid appears thus to be rather well established.

To proceed we now inquire for the possible two-phase coexistence between the fcc HS solid and the HS fluid. To this end we have to solve the following two-phase coexistence conditions

$$p_s(\rho_s)=p_f(\rho_f)\ , \tag{4.17a}$$

$$\mu_s(\rho_s)=\mu_f(\rho_f)\ , \tag{4.17b}$$

expressing the constancy of the pressure (p) and of the chemical potential (μ) (with the temperature providing only a constant scale factor for HS). For the HS solid

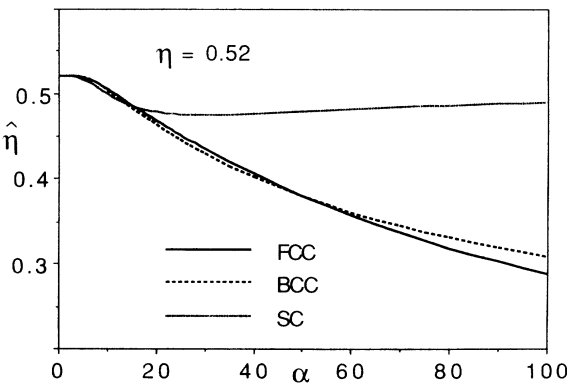

FIG. 4. The packing function of the effective HS fluid ($\hat{\eta}$) vs the Gaussian width order parameter ($\alpha\sigma^2$) of a HS solid of packing fraction $\eta=0.52$ as obtained from the GELA.

$p_s(\rho_s)$ and $\mu_s(\rho_s)$ have been computed as explained in Sec. IV B. Because ρ_f in (4.17) is the actual density of the fluid (which is much larger than the effective density) it is no longer immaterial which HS fluid equation of state is being used. In fact we found that the solution of (4.17) is fairly sensitive to the underlying fluid equation of state (see Table I). Good coexistence data can be obtained from the PY-compressibility equation of state [see (4.3)] but when the much more accurate CS equation of state [see (4.3)] is used the resulting coexistence data become virtually identical to those of the simulation results[21] (see Table I). The full (fluid-fcc solid) HS phase diagram can thus be obtained from the GELA with a high accuracy performing only relatively simple calculations [e.g., only the real space expressions (4.6b), (4.8), (4.12a), and (4.15a) need to be used for the fcc structure]. The only property which is not reproduced accurately by the GELA is the Lindemann parameter L (see Table I). This, however, is a structural property and hence much more model dependent than the thermodynamic properties we did set out to compute. It is not unreasonable to think that the Gaussian approximation (4.6) is the main source of error in the evaluation of L. This however, deserves further study. Notice also that (linearly) extrapolating the high-density behavior of L (see Fig. 5) it is found that L vanishes at $\eta=0.736$ providing hereby a good estimate of the fcc close-packing density ($\eta_{CP}=0.740$).

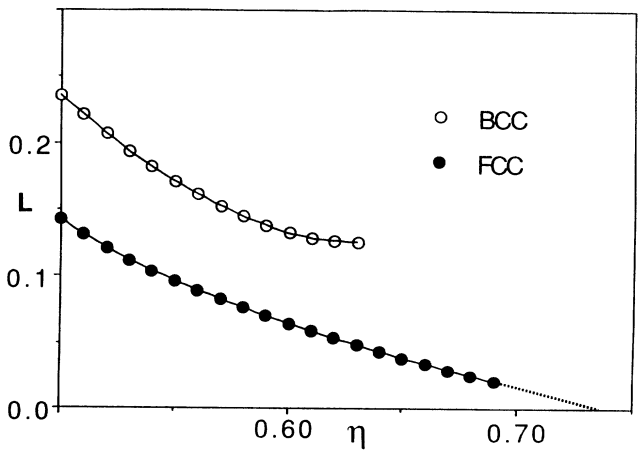

FIG. 5. The Lindemann ratio (L) vs density (η) of the bcc and fcc HS solids as obtained from the GELA. In the Gaussian approximation of Eq. (4.6) we have $L(\text{bcc})=(2/\alpha a^2)^{1/2}$ and $L(\text{fcc})=(3/\alpha a^2)^{1/2}$, with a the lattice spacing and α the Gaussian width order parameter. Notice that extrapolating linearly the fcc values we find $L(\text{fcc})=0$ for $\eta=0.736$ providing hereby a good estimate for the fcc close-packing density ($\eta_{\text{fcc}}=0.740$).

D. The metastable HS solids

Since the HS system is often used as a reference system in the study of more realistic potentials,[4] for which the equilibrium solid is not necessarily a compact structure, it is of some interest to inquire whether the HS potential can also stabilize other crystal structures besides the fcc structure. In the context of the ELA this question has already been investigated[6,15] for the cubic lattices (sc, bcc, fcc). It was found there that the HS potential could not stabilize the sc structure whereas the bcc structure, although stable at high densities, remained metastable with

TABLE I. The fluid-fcc solid coexistence data as computed from the nonperturbative density-functional theories of hard-sphere freezing and compared to the simulation results. Here $\eta=(\pi/6)\sigma^3\rho$ is the packing fraction of the coexisting solid (s) and fluid (f) phases of hard spheres of diameter σ and density ρ. Further, $\Delta\eta=\eta_s-\eta_f$ is the reduced-density change, $\Delta s=s_f-s_s$ the entropy change per particle, $p^*=\beta p\sigma^3$ the reduced pressure at coexistence, and L the corresponding Lindemann parameter [root-mean-square displacement divided by the nearest-neighbor distance; $L=(3/\alpha a^2)^{1/2}$ for a fcc crystal with a being the lattice constant $\rho_s=4/a^3$]. All theories use the PY DCF to describe the solid, while the equation of state used for the fluid is indicated in parentheses [PY or CS; see Eq. (4.3)].

	η_f	η_s	$\Delta\eta/\eta_s$	$\Delta s/k_B$	p^*	L
MC[a]	0.494	0.545	0.094	1.16	11.7	0.126
GELA[b] (CS)	0.495	0.545	0.092	1.15	11.9	0.100
GELA[b] (PY)	0.472	0.522	0.096	1.10	10.3	0.120
SCELA[c] (CS)	0.508	0.560	0.093	1.27	13.3	0.084
SCELA[c] (PY)	0.484	0.538	0.100	1.21	11.2	0.098
WDA[d,e] (CS)	0.480	0.547	0.122	1.41	10.4	0.093
MWDA[e] (CS)	0.476	0.542	0.122	1.35	10.1	0.097
ELA[f] (PY)	0.520	0.567	0.083	1.36	16.1	0.074

[a]From Hoover and Ree (Ref. 21).
[b]From this work.
[c]From Baus (Ref. 9) and this work.
[d]From Curtin and Ashcroft (Ref. 13).
[e]From Denton and Ashcroft (Ref. 12).
[f]From Baus and Colot (Ref. 6).

respect to the fluid phase. In a recent study[22] a stable bcc HS solid was, however, found within the WDA and we will therefore reconsider this question here within the GELA because such relative stability problems are quite sensitive to the approximation scheme. Notice that in the literature one often finds the statement[22] that the bcc HS solid is unstable with respect to shear and hence that Eq. (4.6) can only be used to describe a constrained (shear-stabilized) bcc HS solid. This argument is, however, based on lattice-sum considerations which state[23] that, at zero temperature, the shear modulus of the bcc phase of inverse power potentials $[\sim(\sigma/r)^n]$ of large index $(n \geq 7)$ is negative. It should be stressed here that since the HS system is always pressure stabilized, zero-temperature arguments are strictly speaking not applicable to it. The argument should therefore be reconsidered at finite temperature (or pressure) using, for instance, the DF method to compute the elastic constants of the bcc HS solid in analogy with those calculations[24] already performed for the fcc HS solid. In this case one is probing the stability of the HS solid with respect to changes in its local density which fall outside the class of functions considered in Eq. (4.6) which only probes the stability with respect to particle localization. In the absence of any such calculations (or simulations) we will proceed with Eq. (4.6) to describe the bcc HS solid, leaving open the question whether this solid should be considered as constrained or unconstrained. Contrary to the earlier findings of the ELA,[6] and in agreement with the WDA results,[22] we find from the GELA that the bcc HS solid is metastable relative to the fcc solid but stable relative to the HS fluid for $\eta \geq 0.525$ (see Fig. 2). In the low-density region $(\eta \leq 0.515)$ where both the fcc and bcc solids are metastable relative to the fluid an exchange of stability between fcc and bcc occurs (see Fig. 2) with bcc becoming the most stable phase at low density. Notice also from Fig. 2 that the region of metastability of the bcc phase relative to the fluid extends to lower densities than for the fcc phase. In the region of marginal stability (relative to the fluid) the competition between bcc and fcc is fairly strong. The major difference between the two solids stems from the fact that the bcc solid stabilizes for much lower α values in (4.6) than does the fcc solid. This then implies that in the bcc solid the HS are much more delocalized (see Fig. 5) than is the fcc solid, which is physically reasonable because the bcc structure is a more open structure than the fcc structure. This however has some important consequences for the accuracy of the bcc results. Indeed, from Fig. 4 it is seen that this implies that the effective density describing the bcc solid will be much higher (whereas at constant α these effective densities are comparable) and therefore the results become also much more sensitive to the equation of state of the effective fluid. Our fcc results are thus always more precise than the corresponding bcc results. This problem is particularly important if one wants to resolve the small-α structure of the free energy. An example of the overall

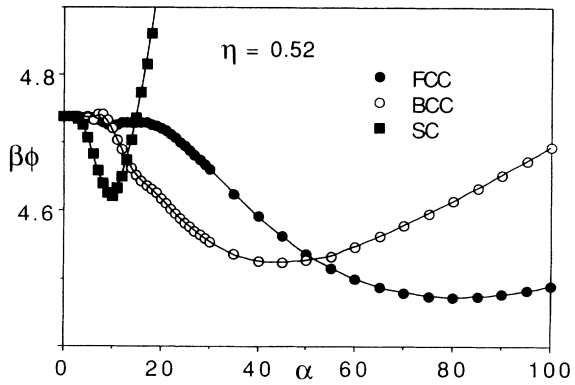

FIG. 6. The reduced free energy per particle $(\beta\phi)$ vs the Gaussian width order parameter $(\alpha\sigma^2)$ of a HS solid of packing fraction $\eta=0.52$ as obtained from the GELA. Notice that, at the free-energy minimum $\alpha(\text{sc}) < \alpha(\text{bcc}) < \alpha(\text{fcc})$ corresponding to an increasing localization of the HS when the lattice becomes more compact, and $\phi(\text{sc}) > \phi(\text{bcc}) > \phi(\text{fcc})$, corresponding to an increasing free-energy barrier separating, respectively, the sc, bcc, and fcc solids from the fluid. This suggests that the equilibrium fluid-fcc solid transition could proceed via the sc and bcc metastable solids.

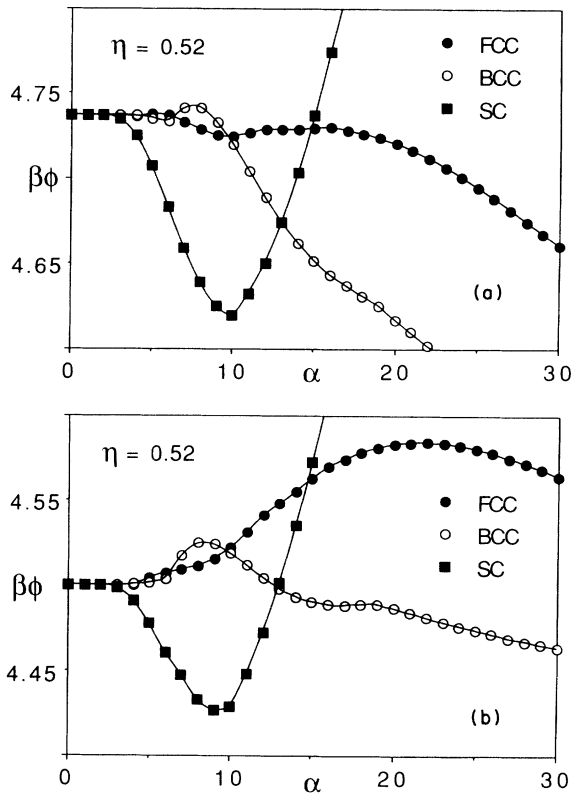

FIG. 7. Enlarged view, in the small-α region, of Fig. 6 showing that the results for the metastable HS solids (sc and bcc) are sensitive to the equation of state of the effective fluid used to describe them. In (a) we show the results corresponding to Fig. 6 and using the usual Percus-Yevick DCF while in (b) we show the results using the DCF of Baus and Colot,[17] with the Carnahan-Starling equation of state build-in. This behavior can be understood by observing that at such small α values the effective densities are still too high (see Fig. 4) for the Percus-Yevick approximation to be valid.

behavior of the free energy versus α is shown in Fig. 6. It is seen there that in the small-α region (i.e., the region before the main valley) some structure develops, including a secondary minimum [see Fig. 7(a)]. Since these α values correspond to fairly large effective densities (see Fig. 4) the details of this structure are largely artefacts of using the PY equation of state for the high-density effective HS fluid. This is illustrated in Fig. 7(b) where an improved DCF, with the CS equation of state build-in, has been used[17] for the effective HS fluid. As a result most of this small-α structure disappears without modifying the large-α behavior. The influence of the underlying fluid equation of state appears to be the largest for the bcc structure. The accuracy of the bcc results is thus somewhat more difficult to access. Unfortunately the information on the bcc HS phase from computer simulations is fairly scarce. If we compare our free energies with the simulation results of Curtin and Runge[22] we find nevertheless a relatively good agreement. For $\rho\sigma^3=1.041$ (1.100) the simulation results for $\beta\phi$ (omitting the $\ln\Lambda^3\rho-1$ term) are[22] 6.094 (6.878) whereas the WDA yields[22] 5.975 (6.771). Here the GELA yields 6.118 (6.991) when the PY DCF is used and 6.049 (6.903) when the improved[17] (CS) DCF is used.

Finally, we have also considered the sc structure. The results follow the same trends as above. The sc structure is metastable with respect to both the bcc and the fcc structure but stable relative to the fluid. At low density, in the region of metastability of the solids relative to the fluid, the sequence is reversed and the sc becomes the most stable of the metastable solids. It also extends to lower densities than the bcc solid. Notice from Fig. 6 that the α value corresponding to the free-energy minimum is very small, pointing to very delocalized particles as physically expected for the very open sc structure. From Fig. 4 it is seen that the effective density of the sc structure is always very high (it saturates at high density). The sc free energy is nevertheless much less affected by the equation of state than the bcc free energy (see Fig. 7). Notice also from Figs. 6 and 7 that the sc freezing is almost second-order-like with an almost vanishing free-energy barrier between the fluid and the solid. In this respect the results obtained here suggest (see Fig. 6) that the fluid-fcc freezing could proceed via a sc-bcc-fcc sequence. Indeed, starting from the fluid and raising the density one first encounters a region where only the sc is (meta)stable. This local free-energy minimum is moreover separated from the fluid by a very small free-energy barrier. Increasing the density somewhat more the bcc phase becomes (meta)stable and the free-energy barrier (i.e., the free-energy maximum separating the bcc minimum from the minimum corresponding to the fluid) is higher than for the sc phase but could easily be reached from the latter. Finally, at higher density the fcc phase becomes (meta)stable with a free-energy barrier which is somewhat larger than for the bcc phase. In this process the HS solid becomes gradually denser and also gradually more localized. It is thus not unreasonable to think that the final nucleation of the equilibrium fcc phase could proceed stepwise via the sc and bcc as intermediate metastable phases. Although we are aware of the fact that the nucleation process depends on more than free-energy considerations, we nevertheless think that this speculation is worthwhile a more complete investigation.

V. CONCLUSION

Between all the recent attempts,[3] aiming at an approximate density-functional description of classical nonuniform equilibrium systems,[1] those based on nonperturbative theories appear to be the most soundly based. We have put in evidence what we think to be the essential ingredient of such theories, namely the mapping of the excess thermodynamics of the nonuniform system onto that of an effective uniform system. This has allowed us to introduce a new and very general theory, the GELA described in Sec. III A, from which most of the remaining theories can be derived by introducing additional assumptions. The predictions of the GELA have been tested here for the description of the hard-sphere solid. The GELA has been found to be very accurate when compared to the simulation results or to other theories. The free energy and pressure of the HS solid depart from the simulation results by less than 3%. Very good fluid-solid coexistence data have also been obtained leading finally to a coherent and accurate picture of the complete HS phase diagram. The theory has a simple formulation and requires only the direct correlation function of the fluid as input. The theory predicts, besides the equilibrium fcc phase, also metastable bcc and sc phases which could play a role in the nucleation of the fcc phase.

ACKNOWLEDGMENTS

One of us (M.B.) acknowledges financial support from the Fonds National de la Recherche Scientifique and also from the Association Euratom-Etat Belge.

[1] R. Evans, Adv. Phys. **28**, 143 (1979) and references therein.
[2] R. Evans, in *Liquids at Interfaces,* edited by J. Charvolin, J. F. Joanny, and J. Zinn-Justin (Elsevier, Amsterdam, 1989).
[3] M. Baus, J. Stat. Phys. **48**, 1129 (1987); A. D. J. Haymet, Ann. Rev. Phys. Chem. **38**, 89 (1987); M. Baus, J. Phys.: Condens. Matter **2**, 2111 (1990).
[4] J. P. Hansen and I. R. McDonald, *Theory of Simple Liquids* (Academic, London, 1976).
[5] See, e.g., J. L. Colot, X. G. Wu, H. Xu, and M. Baus, Phys. Rev. A **38**, 2022 (1988).
[6] M. Baus and J. L. Colot, Mol. Phys. **55**, 653 (1985).
[7] W. A. Curtin, J. Chem. Phys. **88**, 7050 (1988).
[8] T. V. Ramakrishnan and M. Yussouff, Phys. Rev. B **19**, 2775 (1979).
[9] M. Baus, J. Phys.: Condens. Matter **1**, 3131 (1989).
[10] J. F. Lutsko and M. Baus, Phys. Rev. Lett. **64**, 761 (1990).
[11] J. L. Barrat, J. P. Hansen, and G. Pastore, Phys. Rev. Lett. **58**, 2075 (1987); W. A. Curtin and N. W. Ashcroft, Phys. Rev.

Lett. **59**, 2385 (1987); A. R. Denton and N. W. Ashcroft, Phys. Rev. A **39**, 426 (1989).
[12]A. R. Denton and N. W. Ashcroft, Phys. Rev. A **39**, 4701 (1989).
[13]W. A. Curtin and N. W. Ashcroft, Phys. Rev. A **32**, 2909 (1985).
[14]P. Tarazona, Mol. Phys. **52**, 81 (1984); Phys. Rev. A **31**, 2672 (1985).
[15]J. L. Colot and M. Baus, Mol. Phys. **56**, 804 (1985); J. L. Colot, M. Baus, and H. Xu, Mol. Phys. **57**, 809 (1986).
[16]M. Popovic and M. V. Jaric, Phys. Rev. B **38**, 808 (1988).
[17]M. Baus and J. L. Colot, Phys. Rev. A **36**, 3912 (1987); for HS see Eq. (3.35) and (2.22) herein.
[18]D. Frenkel and A. J. C. Ladd, J. Chem. Phys. **81**, 3188 (1984).
[19]See K. R. Hall, J. Chem. Phys. **49**, 3609 (1986).
[20]D. A. Young and B. J. Alder, J. Chem. Phys. **60**, 1254 (1974).
[21]W. G. Hoover and F. M. Ree, J. Chem. Phys. **49**, 3609 (1968).
[22]W. A. Curtin and K. Runge, Phys. Rev. A **35**, 4755 (1987).
[23]W. G. Hoover, D. A. Young, and R. Grover, J. Chem. Phys. **56**, 2207 (1972).
[24]See, e.g., H. Xu and M. Baus, Phys. Rev. A **38**, 4348 (1988).